

Three-particle quantum correlation interferometry

F.V. Kowalski

Physics Department, Colorado School of Mines, Golden CO. 80401 U.S.A.

A three-body quantum correlation is calculated for two particles reflecting from a mirror. Correlated interference, a consequence of conservation of energy and momentum, occurs for states in which the order of reflection is indeterminate. The resulting quantum joint probability density function exhibits interference with diverse characteristics, depending on the coherence lengths of the substates. Marginal probability density functions can contain information about the quantum nature of all three bodies, even if only one particle is measured. Two microscopic particles reflecting from a mesoscopic mirror are used to illustrate unique features of this three-body correlation interferometry. The microscopic momentum exchanged then generates mirror substates which interfere to produce quantum effects which do not vanish with increasing mirror mass, while the small displacement between these mirror states can yield negligible environmental decoherence times.

PACS numbers: 03.65.Ta, 03.65.-w, 03.75.Dg, 03.75.-b

Multiparticle interferometry generates both many-body quantum correlations, which depend on the number of paths and/or the number of particles within such an interferometer[1], and marginal probability density functions. For bipartite systems, using photon pairs generated by parametric downconversion, various interferometer paths have been used [1–4]. However, experimental confirmation of quantum predictions is more difficult to obtain for similar systems with non-zero rest mass particles.

Scarcer yet are examples of three-body interferometers, although gedankenexperiments (typically using identical particles) have been discussed [1, 5]. This is perhaps due to a combination of few exact solutions for three-body systems and the difficulty in constructing three-body beamsplitters.

Here, both a three-body beamsplitter and interferometer are described using three distinguishable non-zero rest mass particles. The splitting mechanism involves elastic reflection in one dimension. By increasing the number of interacting particles, this reflection process can act as a beamsplitter or interferometer for even more particles. Measurements of particle reflection, but not associated with interference, have involved mirrors that reflect atoms [6] and Bose-Einstein condensates [7], atoms reflecting from a solid surface [8], neutrons [9] and atoms [10] reflecting from vibrating mirrors, and atoms reflecting from a switchable mirror [11].

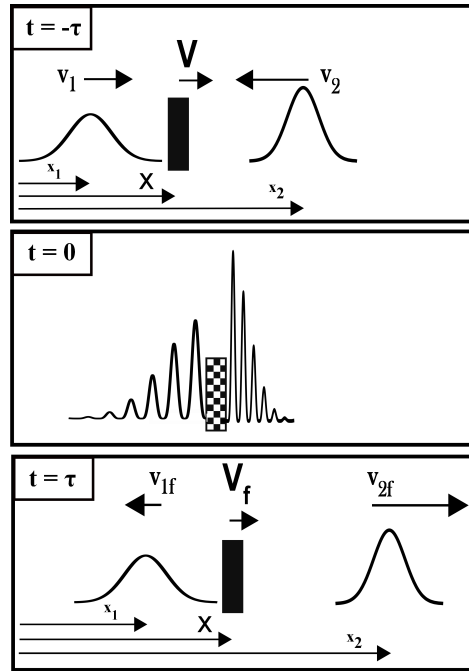


FIG. 1: 3-body reflection schematic.

Fig. 1 shows schematic representations of this 3-body state splitting process. Actual three-body quantum joint probability density functions, PDFs, are described later. The particle substate PDFs, before interaction, are the Gaussians at $t = -\tau$, one of which, to the left of the ‘mirror’, is moving to the right, while the other, to the right of the ‘mirror’, is moving to the left. The ‘mirror’ is represented as the black rectangle, moving to the right. These are referred to as particle 1, the mirror, and particle 2, with masses m_1, M, m_2 , initial velocities v_1, V, v_2 , and coordinates x_1, X, x_2 , respectively.

At $t = 0$ interference between the incident and reflected particle substates is shown as oscillations in the PDF, while interference between the mirror substates, which have and have not reflected the particles, is represented by the rectangular checkerboard pattern rather than the solid rectangle. This snapshot at $t = 0$ illustrates a region of correlated interference, although the correlation cannot be shown in such a simple schematic. These quantum correlations in the three-body interference, a consequence of conservation of energy and momentum, are manifest as coincidence rates, e.g. a correlation in the measurement of the positions of the particles and mirror. A null in the PDF, as a function of the three coordinates, is an example of a correlation where all three objects cannot be observed. At time $t = \tau$ the three wavegroups have separated so that no overlap occurs. The expectation value of the position of each wavegroup substate then obeys the laws of classical reflection.

Fig. 1, at $t = 0$, illustrates an ‘open-interferometer,’ where the phase difference, which determines interference, depends on the spatial locations and times of measurement of each particle in the multiparticle system. A one-particle example of such an open interferometer is the region behind a double slit, where the detector’s output depends on its location. The phase difference in a closed interferometer, such as a one-particle Mach-Zehnder, depends on its fixed path difference and is independent of the detector location beyond the output port. A gedankenexperiment for a three-particle closed interferometer is found in reference [1].

Detection of the three objects, in fig. 1, can then occur at different times and locations, yielding asynchronous correlation interferometry [12]. Here, however, only synchronous measurement is considered [13].

Assume that the two particles and mirror are initially in an uncorrelated eigenstate of energy before reflection. The three-body Schrödinger equation for reflection is then solved for the energy eigenstates. Wavegroups, as sketched in fig. 1, are formed from a superposition of these solutions. The particle-mirror interaction is modeled as a moving delta function potential where reflection is assumed to occur at the center of mass of the mirror, with the boundary condition that the wavefunction (incident and reflected states) vanish at $x_1 = X = x_2$.

Consider next the energy eigenstates for the system shown in fig. 1. These three bodies can exist in 6 possible eigenstates: **(1)** uncorrelated incident, **(2)** particle 1 has reflected but not particle 2, **(3)** particle 2 has reflected but not particle 1, **(4)** particle 1 reflected first followed by reflection of particle 2, **(5)** particle 2 reflected first followed by reflection of particle 1, and **(6)** simultaneously reflection of the three bodies. Since it is not known where the bodies are located for energy eigenstates, the amplitudes for these six ‘paths’ must be summed.

Interestingly, conservation of energy and momentum do not determine a unique solution for simultaneous 3-body elastic reflection [14]. It is assumed here that the probability for such a collision is small compared with that of the other five ‘paths’ and therefore is neglected [15]. Experimental confirmation of the resulting predictions will validate this assumption.

Generic results are too lengthy to present. However, in the limit $M \gg (m_1, m_2)$, the PDF for the wavefunction, which is the sum of these energy eigenstates, reduces to

$$PDF_{eigenstate}^{energy} \propto \frac{3}{2} - \cos(\alpha) + \frac{\cos(\alpha + \beta)}{2} - \cos(\beta), \quad (1)$$

with

$$\alpha = \frac{2m_1(V - v_1)(x_1 - X)}{\hbar} \quad \text{and} \quad \beta = \frac{2m_2(V - v_2)(X - x_2)}{\hbar}.$$

Note that the parameters of the three bodies are coupled in this interference expression.

To understand why the fringe spacing in eqn. 1 is independent of M , consider reflection of only one microscopic particle from a nearly stationary mesoscopic mirror. In addition, approximate this two-body state as two one-body states, one for the particle and the other for the mirror. The mirror state is then a superposition of mirror wavefunctions before and after reflection. The phase difference between these mirror states is $\Delta K X$, where ΔK is their wavevector difference. The mirror fringe spacing is only determined by the change in particle momentum since conservation of momentum in reflection requires $\Delta K = \Delta k$, where Δk is difference in particle wavevectors between reflection and no reflection. The particle and mirror fringe spacings are therefore the same. While this simplified model, reducing a two-body state into two one-body states, demonstrates why interference for a mesoscopic mirror mass does not become imperceptible as $m/M \rightarrow 0$, it does not account for the correlation given in eqn. 1, which is intrinsically a many-body effect.

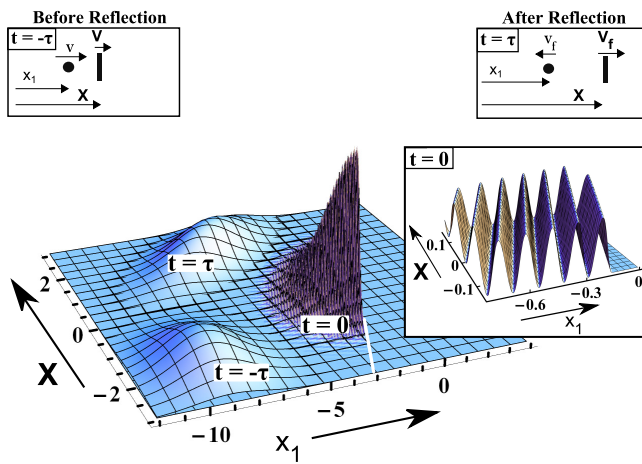


FIG. 2: Three sequential two-body joint probability density snapshots vs coordinates (x_1, X) for only reflection of particle 1 from the mirror. The lower PDF waveform moves toward the diagonal white line, corresponding to $x_1 = X$, then reflects in the middle snapshot where the incident and reflected two-body wavefunctions ‘overlap’, and finally it moves away from the diagonal in the upper snapshot. The upper left inset is a schematic of the ‘classical’ analog before reflection while the upper right inset is that after reflection. The middle right inset is a magnified version of the $t = 0$ plot. There is no classical analog for the middle snapshot.

Double slit interference with a mesoscopic particle, on the other hand, superposes two one-body states with the same momentum whose difference in phase in the far field, $k\Delta x$, is due to the difference in path lengths from each slit to the measurement point times an extremely large wavevector. This results in an imperceptible fringe spacing.

Any experimental realization of such an interferometer will involve wavegroups, which are formed by summing over these energy eigenstates for Gaussian distributions of the initial velocities of the mirror and particles. A generic analytic expression for a 3-body wavegroup, used in the figures below, can be obtained if all three are measured simultaneously.

Fig. 2 illustrates the PDF for reflection of *only* particle 1 from the mirror. This is represented schematically in fig. 1 by eliminating particle 2.

It is difficult to display PDF plots of correlated interference, as shown schematically in fig. 1, when particle 2 also reflects. Instead, these plots are shown below as a function of only the coordinates of particle 1 and the mirror, for a fixed position of particle 2. Another simplification, to illustrate such 3-body PDFs, incorporates a broadband mirror substate wavegroup (narrow spatial width compared with the fringe structure) with narrow band (large spatial width compared with the fringe structure) particle substate wavegroups. This transforms the wavegroup shown in fig. 2 into one with an elliptical footprint in the (x_1, X) plane, whose large major and small minor axes are along x_1 and X , respectively.

The interferometric effects of the addition of the third body are then shown in fig. 3 for the snapshot at $t = 0$. The only difference between the upper and lower two plots in fig. 3 is the value of x_2 . In both plots, x_2 is fixed to be within the position of interferometric PDF oscillations sketched in fig. 1. The lower horizontal ridge along the x_1 axis corresponds to a superposition of the incident wavegroup with and without having reflected particle 2. The diagonal oscillations in the PDF correspond to a superposition of paths (2), (4), and (5), which are defined above. This is a manifestation of the 3-body interferometer.

A PDF plot for reflection of only particle 1 from the mirror, with the same parameters as used in the upper and lower plots of fig. 3, is shown in the inset at the middle of fig. 3. Only two PDF ridges appear, with no oscillations. There is also no 2-body interference, as shown in the middle snapshot of fig. 2, since the short spatial width of the mirror wavegroup substate, relative to its recoil distance, now results in distinguishable two-body states (the particle and mirror have reflected for the diagonal ridge but not for the horizontal ridge).

Fig. 4 illustrates reflection acting more as a beamsplitter than an interferometer. This is accomplished by narrowing the spatial width of the mirror substate wavegroup while also increasing the mass of particle 2, relative to the parameters used in fig. 3. The reflection of particle 2 then imparts sufficient momentum to separate these narrower

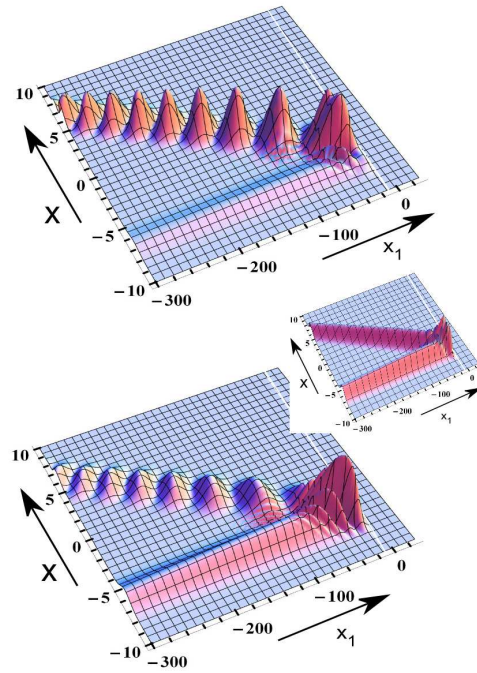


FIG. 3: Reflecting wavegroup with an elliptical footprint in the (x_1, X) plane. The parameters in the upper and lower 3-body PDF correlated interference plots differ only by the particular value used for x_2 . Using the same parameters, the inset shows a 2-body PDF plot for reflection only of particle 1 from the mirror.

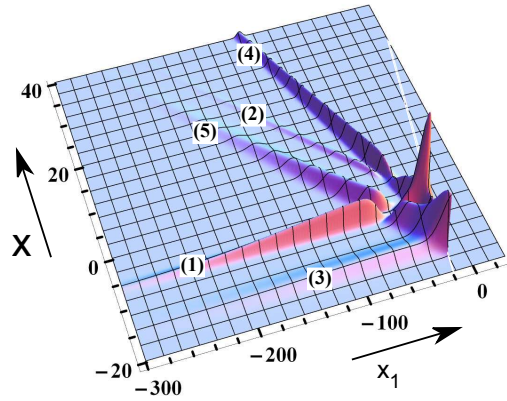


FIG. 4: Fig. 3 has been modified by increasing m_2 and decreasing the spatial width of the mirror. The paths associated with the separate ridges are labeled as described in the text. The lack of overlap prevents the interference shown in fig. 3.

wavegroups, thereby eliminating the interference shown in fig. 3. For example, the two interfering states parallel to the x_1 axis of fig. 3, corresponding to paths **(1)** and **(3)**, no longer overlap in fig. 4. For a measurement of particle 1 at x_1 and particle 2 at the value used in the figure, the mirror is split into 5 distinct positions along the ridges, each associated with a path, labeled numerically, as defined above. Although the different paths no longer overlap, this is not a separable state.

Verification of such correlated interference requires simultaneous measurement of both particles and the center of mass of the mirror with instruments having a spatial resolution smaller than the fringe spacing. For a static mesoscopic mirror reflecting microscopic particles, this spacing is about half the deBroglie wavelength of the particles, which at $\sim 1 \mu\text{m}$ for ultracold atoms [16], potentially satisfies this requirement. Additionally, the effects of the longitudinal

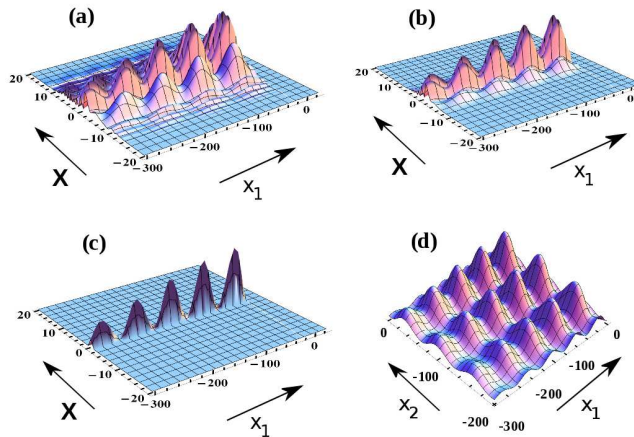


FIG. 5: Plots (a) through (c) show decreasing mirror coherence lengths, with x_3 and the coherence lengths of both particles fixed. Part (d) illustrates the marginal PDF derived from part (c).

coherence length, l_c , need to be considered. For ultracold atoms $l_c \leq 10 \mu\text{m}$ [16], while for a mirror this is given by $l_c \approx \lambda^2/\Delta\lambda = \lambda V/\Delta V$ [17]. If the uncertainty in the mirror velocity is determined by its thermal equilibrium with the environment then $\Delta V_{\text{thermal}} \approx \sqrt{2k_B T/M}$ yielding for the mirror, $l_c^{\text{thermal}} \approx h/\sqrt{2Mk_B T}$.

A sequence of 3-body PDFs in the correlated interference region is shown in figs. 5 (a), (b), and (c), with coherence lengths for the mirror progressing from larger to smaller than that shown in fig. 3. The particle masses have also been decreased, relative to those used in fig. 3, to impart insufficient momentum to separate these narrower wavegroups, thereby generating the interference similar to that shown in the middle snapshot of fig. 2.

Measuring correlations among fewer bodies is more practical. To predict such results, the many-body PDF is integrated over the coordinates of one or more of the bodies, appropriately reducing the coordinate space that the PDF spans and yielding a marginal PDF [5]. For example, integrating over the mirror coordinate reduces $\text{PDF}(x_1, \mathbf{X}, x_2)$ to $\text{PDF}(x_1, x_2)$. This procedure, when applied to the PDF shown in fig. 5 (a), virtually eliminates interference. Yet, for the conditions illustrated in fig. 5 (c), this leads to the marginal $\text{PDF}(x_1, x_2)$ shown in fig. 5 (d).

For these long coherence length particle substates and the short coherence length mirror, this marginal PDF can be approximated, using eqn. 1, with the mirror substate being a delta function distribution in position, peaking at $\mathbf{X} = \mathbf{X}_0$. Integrating over the mirror coordinate then yields $\text{PDF}_{\text{eigenstate}}^{\int \dots d\mathbf{X}}(x_1, x_2) = \text{PDF}_{\text{eigenstate}}^{\text{energy}}(x_1, \mathbf{X}_0, x_2)$. This differs from the result shown in fig. 5 (d) by a slight variation in the magnitude of the PDF due to the large but finite particle coherence lengths.

A comparison of $\text{PDF}_{\text{eigenstate}}^{\int \dots d\mathbf{X}}(x_1, x_2)$ can be made with independent one-body solutions to the Schrödinger equation with $M \gg (m_1, m_2)$ (one solution for each particle residing on opposite sides of the mirror) while treating the mirror as a classical potential. The resulting PDF, with $\mathbf{X} \rightarrow \mathbf{X}_0$ in α and β ,

$$\text{PDF}_{\text{mirror}}^{\text{classical}}(x_1, x_2) \approx 2 - \cos(\alpha) - \cos(\beta), \quad (2)$$

differs from the approximate marginal PDF by not having the correlation term $\cos(\alpha + \beta)$ (which adds a phase shift and a variation in the magnitude of the PDF as a function of position).

A measurement might then consist of ultra cold atoms reflecting from opposite sides of a stationary mirror. Observation of a standing wave atom PDF pattern, with the correlation term, would then indicate quantum behavior of the mirror without a direct measurement of it.

While the approximation using eqn. 1 is useful in understanding how the interaction of the three bodies is manifest in a marginal PDF, it is incomplete for short coherence length particle substates since both the time dependent motion of the wavegroup and its spatial dependence are neglected. It is most accurate during overlap of the wavegroups.

The coordinate space of $\text{PDF}(x_1, x_2)$ can again be lowered by reducing the coherence length of particle 2, resulting in a sequence for fig. 5 (d) which progresses in a similar manner to fig. 5 (a) going to fig. 5 (c). The particle 2 substate then becomes a delta function distribution in position, peaking at $x_2 = x_{20}$ while that of particle 1 remains in a broad spatial distribution. This one body PDF can again be approximated by integrating $\text{PDF}_{\text{eigenstate}}^{\int \dots d\mathbf{X}}(x_1, x_2)$

over x_2 yielding,

$$PDF_{eigenstate}^{\int \dots dX dx_2}(x_1) \propto \frac{3}{2} - \cos(\alpha) + \frac{\cos(\alpha + \beta)}{2} - \cos(\beta), \quad (3)$$

with $X \rightarrow X_0$ and $x_2 \rightarrow x_{20}$ in α and β .

Such a result is useful in estimating the 3-body correlation effects in the one-body marginal PDF. However, the approximation again neglects the time evolution and spatial dependence of the wavegroup substates. The validity of this approximation then rests on the order of reflection being indeterminate. The long duration of the particle 1 interaction mitigates this constraint.

If, on the other hand, the particle 2 wavegroup reflects before or after any interaction of particle 1 with the mirror, then the result is the one-body solution to the Schrödinger equation, $PDF_{mirror}^{one\ body}(x_1) \propto 1 - \cos(\alpha)$. This differs from the 3-body result given by eqn. 3 by the correlation term.

By measuring neither the mirror nor particle 2, evidence of 3-body superposition can therefore be retained in the measurement of the standing wave PDF of only particle 1. Such a measurement might consist of a nearly static mirror in a system with coherence lengths $l_c^M \ll l_c^{m_2} \ll l_c^{m_1}$. A fixed delay of particle 2 (constant β due to a fixed $x_2 - X$) is introduced. The interaction time of particle 1 must be longer than the transit time of particle 2 to the mirror for the order of reflection to remain indeterminate. Observation of the correlation term in only the standing wave PDF pattern for particle 1, as a function of $x_1 - X$ (and therefore α), would then indicate quantum behavior of the mirror.

Correlation interferometry in reflection has advantages in measuring many-body quantum effects both on systems composed of 3 or more bodies and on mirrors of increasing mass. There is neither the alignment nor the path length sensitivity found in division of amplitude or wavefront interferometers, while the beamsplitting mechanism requires only that the order of reflection be indeterminate. In addition, many body effects can remain in the marginal PDF. Therefore, it is interesting to determine the upper limit on the mirror mass in observing such quantum correlations.

Mesoscopic superposition states have been of concern since early in the development of quantum mechanics. To understand why such states can potentially be observed, some assumptions about arguments against such observations need to be challenged in relation to the example treated here. A summary, including results from more detailed treatments on two-body reflection [12, 13], is: (1) The mirror fringe spacing does not shrink as its mass increases due to the superposition of mirror states which differ only by the microscopic momentum exchanged with the particles. (2) Interferometric quantum correlation is a requisite in satisfying conservation of energy and momentum in reflection. (3) The difference in wavevectors of the interfering mesoscopic mirror substates, due to reflecting microscopic particles, divided by the spread in wavevectors, of which the mirror substate is composed due to thermal motion, is the ratio R . Optical wavegroups with R values similar to a microscopic particle reflecting from a mesoscopic mirror have been shown to exhibit interference. (4) Decoherence of the mesoscopic superposition via interaction with the environment increases exponentially with the spatial separation of these states [18]. The small separation of these interfering mesoscopic mirror states, having reflected microscopic particles, mitigates such decoherence. (5) Many-body quantum effects are maintained for short mirror coherence lengths, even in the marginal PDF, as shown above. (5) The robust character of interference for objects with many degrees of freedom is reinforced by measurements which demonstrate that even if the size of the object is larger than both the coherence length and deBroglie wavelength, interference can still be observed [16].

Only a small set of parameters and interferometric geometries have been explored here. Other possibilities include closed interferometers, such as a thin aluminum film generating reflections of a neutron from both its surfaces [12]. Such interference is not transient for the same reasons that occur in optical pulse reflection from a thin film. Reflection of two neutrons from such a film is potentially a more feasible extension of the 3-body correlated interference work described here. Asynchronous measurement in many body systems can also mitigate transient interferometric effects [12].

Reflection of atoms from mirrors has been previously studied, but not in treating both the particle and reflector as quantum objects, nor in the mesoscopic reflector mass regimes considered here, nor in an attempt to measure the resulting 'standing-wave' interference. There exist few examples of 3-body quantum correlated interference for non-zero rest mass particles. Verification of the above predictions, even in the microscopic regime for both particles and mirror, is therefore of fundamental interest. Although neither comprehensive nor intended as an experimental proposal, these results indicate a direction, heretofore unexplored, for further research in understanding many body

quantum correlations and extending quantum measurements to larger masses.

- [1] D. M. Greenberger, M. A. Horne, and A. Zeilinger, *Physics Today* **46** 22 (1993).
- [2] D. Franck, *Phys. Rev. Lett.*, **62** 2205, (1989).
- [3] J-W. Pan, D. Bouwmeester, M. Daniell, H. Weinfurter, and A. Zeilinger, *Nature*, **403** 515, (2000).
- [4] J-W. Pan, Z-B. Chen, C-Y. Lu, H. Weinfurter, A. Zeilinger, and M. Żukowski, *Rev. Mod. Phys.* **84**, 777.
- [5] K. Gottfried, *Am. J. Phys.* **68** 143 (2000).
- [6] D. Kouznetsov and H. Oberst, *Phys. Rev. A* **72**, 013617-1 (2005).
- [7] T. A. Pasquini, M. Saba, G.-B. Jo, Y. Shin, W. Ketterle, and D. E. Pritchard, *Phys. Rev. Lett.* **97**, 093201-1 (2006).
- [8] F. Shimizu, *Phys. Rev. Lett.* **86**, 987 (2001).
- [9] T. Hils et. al., *Phys. Rev. A* **58**, 4784 (1998).
- [10] Y. Colombe, B. Mercier, H. Perrin, and V. Lorent, *Phys. Rev. A* **72**, 061601 (2005).
- [11] Szriftgiser, P., D. Guery-Odelin, M. Arndt, and J. Dalibard, *Phys. Rev. Lett.* **77**, 4 (1996).
- [12] A two-body treatment of asynchronous measurement in reflection is found here: Kowalski, F.V. and R.S. Browne, *Foundations of Physics*, 11/2015; DOI:10.1007/s10701-015-9965-7
- [13] A two-body treatment of synchronous measurement in reflection is found here: Kowalski, F.V. and R.S. Browne, arXiv:1404.7160
- [14] B. Smith, et. al., *ACM Transactions on Graphics (Proceedings of SIGGRAPH 2012)*, **31**, 186:1 (2012).
- [15] Quantum correlation in a simultaneous 3-body collision is then determined by more than just the conservation laws.
- [16] A. D. Cronin, J. Schmiedmayer, and D. E. Pritchard, *Rev. Mod. Phys.* **81**, 1051 (2009).
- [17] M. Ferrero and A. van der Merwe, *Fundamental Problems in Quantum Physics*, p-125 (Kluwer Academic Publishing, Dordrecht, 1995).
- [18] W. H. Zurek, *Rev. Mod. Phys.*, **75**, 715, (2003).